3D printing in medicine; Application in Intracranial Tumours in Southern Nigeria

Abstract

Background

The pituitary gland is a small bean-shaped gland situated at the base of the brain. Pituitary-based tumors are neuroendocrine tumours affecting the pituitary gland. Imaging of the pituitary gland involves the use of computed tomography and magnetic resonance imaging. 3D reconstruction of data from CT images can be converted into 3D and then made into a live anatomical model using a 3D printer.

The objective and aim of this study are to demonstrate that findings from CT scan images can be used to generate 3D printed specific models for patients and clinicians.

Methods

Patient-specific models for three clinical cases were segmented using a segmentation application to isolate the mass and the bone. The process involved image acquisition from a cross-sectional imaging to segmentation of the acquired DICOM image into a 3D model followed by file and model correction for final print, this is then followed on to slicing with the selection of 3D printing material as well as appropriate settings, this is then concluded with the actual print, print accuracy, and cost analysis.

Results

Segmentation of the region of interest took about 45 to 90 minutes with the majority of the time spent on segmentation of the pituitary. Printing of models was done into sections as the

skull and mass were printed separately. The times required spanned from 20-40 minutes and 4-9 hours for the mass and skull base respectively. Print accuracy was less than 1.7mm with the total cost of printing a model was less than $50.

Conclusion

This study showed steps in 3D printing anatomical models from a computed tomogram of patients with brain lesions.

Keywords: 3D printing, accuracy, Digital Imaging and Communications in Medicine (DICOM), intracranial tumours, pituitary gland, segmentation

Introduction

The pituitary gland is a small bean-shaped gland situated at the base of the brain and composed of three distinct histological parts. It produces several hormones that control other endocrine glands(1). These hormones include adrenocorticotropic hormone (ACTH), thyroid-stimulating hormone (TSH), growth hormone (GH), luteinizing hormone (LH), and follicle-stimulating hormone (FSH). Oxytocin and arginine vasopressin are also released secondarily. These hormones regulate several physiological processes, such as cardiovascular, metabolic and reproductive.(1)

The pituitary gland is located within the pituitary fossa with complex relationships. Inferiorly, it is bounded by the sphenoid sinus, superiorly, by the diaphragm sellae, laterally by the cavernous sinus, anterior clinoid processes, and posteriorly by the posterior inter-cavernous sinus and dorsum sellae (2).

Tumours affecting the pituitary —both adenomas and carcinomas— are neuroendocrine and are one of the most common intracranial tumours (3). Pituitary adenomas are usually classified into micro□ and macroadenomas, the latter being defined by a size greater than 10 mm, while microadenomas are smaller than this. However, this differentiation is regarded as arbitrary(4). Studies show pituitary adenomas are common and account for approximately 10% of intracranial tumours and 30-50% of all pituitary region masses(3,5). Autopsy and radiology studies have shown that between 10% and 20% of all pituitary tumours may be incidental(6).

In evaluating pituitary tumours, magnetic resonance imaging (MRI) is the preferred modality to assess the pituitary gland and surrounding structures. Other alternative imaging strategies to

aid visualization are Positron Emission Tomography (PET) with Computed Tomography (PET/CT) or MRI (PET/MR) which permit correlation of function and anatomy. Incidental pituitary tumours, however, are discovered on CT which further prompts the use of MRI in evaluation(7,8).

Treatment recommendations for pituitary tumours range from no immediate treatment, to medical or surgical treatment. Surgical treatment, however, is the mainstay of treatment(7). Surgical approaches like the minimally invasive transsphenoidal approach which is regarded as safe, versatile, and effective in about 95% of pituitary tumours(9). Difficulties like incomplete resection may occur depending on various factors like the size of the tumour, proximity to vital structures such as the neurologic structures, carotid arteries, and the cavernous sinuses located adjacently. Surgery poses other risks. Mortality, which is the least of them accounts for less than 0.5%, however major complications like CSF leak, meningitis, ischemic stroke, and intracranial haemorrhage can occur. Furthermore, minor complications like sinus disease, septal perforations, epistaxis, wound infections and hematomas also can occur(9).

Treatment of pituitary tumours usually requires a detailed multidisciplinary approach to planning the patient's management. The multidisciplinary team (MDT), may comprise of clinicians from various disciplines, including endocrinology, neurosurgery, radiology, and otolaryngology [ear, nose, and throat (ENT)], to determine suitability for surgery and inform the choice of surgical approach.

Three-dimension construction of cross-sectional medical images involve the use of stacked 2D Digital Imaging and Communications in Medicine (DICOM) images from cross-sectional imaging modalities like MRI and CT. DICOM images are the leading standard in the medical imaging field (10). DICOM images are converted to 3D computer-aided design (CAD) data. Out of the about 100 file formats of 3D CAD files used as native 3D data, stereolithography or Standard Tessellation Language (STL) file format is the most commonly used for 3D printing (11). There are commercial and open-source software packages for the segmentation of DICOM images to STL data, all of which run on a general-purpose personal computer (PC). Examples include 3D slicer, 3D view, Image J, Mimics, InVesalius 3, OsiriX lite, Seg3D, etc. However, some imaging workstations provided by companies (e.g. General electronics) that produce image scanners now have software available for converting DICOM to STL files (12).

3D printing systems come in various forms like Fused deposition modelling (FDM), Stereolithography(SLA), Digital Light Processing(DLP), Selective Laser Sintering (SLS), Selective laser melting (SLM), Laminated object manufacturing (LOM), and Digital Beam Melting (DBM) (13). FDM printers/technology is currently the most popular 3D printing technology and is used in both affordable 3D printers and even 3D pens(13).

Applications of 3D printing from cross-sectional images like MRI and CT have shown great importance in several surgical practices such as surgical planning, implant preplanning, and enhance patient understanding of the condition and surgical process (14). Guidelines and applications for use of 3D printing have been developed in clinical practice, including,

maxillofacial, orthopaedics, cardiac and hepatobiliary, and other conditions where it may have a potential role in informing management.

In this work, we aim to demonstrate that findings from CT cross-sectional images of several patients can be used to produce 3D printed patient-specific models. We showed the process involved in 3D printing a brain tumour. Lastly, we compared the accuracy of the 3D prints with the cross-sectional images acquired and did a cost analysis to determine its feasibility.

Methods.

Imaging

CT scans were acquired with GE CT scanners in a radiological centre in southern Nigeria. Images were reconstructed using a 3D slicer. 3D slicer is a desktop software application for the visualization and analysis of medical images and computing data sets. DICOM images were exported to a PC and then segmented to a 3D surface model. CT head of 3 patients were obtained with scanning parameters shown in table 1;

Table 1: Imaging findings and biodata of identified Cases

Case	Age (years)	Sex	Slice thickness	Imaging findings

Case 1	25 years	Male	1.25mm	Contrast-enhanced lobulated mass in the pituitary fossa with multifocal areas of hyper-density of calcific attenuation. Mass is seen eroding anterior and posterior clinoid processes
Case 2	7 years	Female	5mm	Large calcified wedge-shaped mass merging imperceptibly with the pituitary fossa and the clinoid processes in the pituitary fossa. There is associated obliteration of the aqueduct of Sylvius with resultant dilatation of the 3rd and lateral ventricles
Case 3	52 years	Female	3.75mm	Irregularly shaped contrast enhancing hyperdense solid mass with calcifications arising from the Sella with an adjacent cystic component extending into the suprasellar space. The mass is infiltrating the sphenoidal sinus, eroding into the sphenoid bone, part of the right petrous, temporal bone as well as the anterior and posterior clinoid processes bilaterally but worse on the right.

Image segmentation and model preparation for 3D printing.

The CT DICOM images were collected and loaded onto the 3D slicer software. Segmentation of the skull was achieved using Hounsfield unit (HU) values between 100HU and 1000HU. Small floating structures within this segmentation were removed using the 'Islands' and 'scissors' tools. In the segmentation of the tumour, two segments were used- that of the tumour and other tissue. This tumour was then selected using the 'paint' tool. The paint seed was placed within the tumour and on the normal tissue around the tumour. The 'grow from seeds' is then selected to initialize automatic region growing and then show a 3D presentation of the tumour. The resultant segmentation is refined by painting the areas not selected by the automatic

region growing. Some smoothing is done to reduce the segmented surface. Median smoothing filter of 3mm was used to smoothen the structures. The image generated is then reassessed to check if the edges of the tumour are covered. The final segments are then exported into an STL file with a scale of 0.3 to 0.5. The final STL file was transferred to a creality slicer application which converts the 3D object model to specific instructions for the printer. The converted version from the STL is processed in the g-code format used by the fused filament 3D printer. The 3d slicer parameters used include an infill of 10-20%, extrusion thickness of 0.2mm, and presence of support as well as brim for adhesion to the print bed. The minimal support material was however used to reduce print time and the need for post-processing of the 3D printed models. Printing was used with a consumer-available 3D printer, Creality Ender 3 pro v2. PLA filaments were used to print using a layer height of 0.2 mm and a 0.4 mm nozzle.

Cost analysis

The cost of production of each model was divided into two, the cost of time spent at segmentation and the cost of PLA material used to print the model. The cost of PLA material was calculated from the purchase price of the filaments and the weight of the final 3D printed model. The personnel cost was estimated to be about $23 per hour.

Figure 1: Steps/workflow in developing a 3D print from acquired image results

Results

Segmentation of the region of interest took about 45 to 90 minutes with the majority of the time spent on segmentation of the pituitary tumour. This was made easy with the IV contrast enhancement and calcifications of the mass. Segmentation of the bony structures is required using a near automated thresholding technique.

Printing of models was done into sections as the skull and mass were printed separately. The times required spanned from 20-40 minutes and 4-9 hours for the mass and skull base respectively.

Table 2a: Print accuracy of 3D printed anatomical model

Case	Mass (3D printed) (mm)	Mass (CT image) (mm)	Mass (3D printed with scaling) (mm)	Difference (mm)
Case 1	18.3	35.0	36.6	1.6
Case 2	21.7	44.3	43.7	0.6
Case 2 (dilated ventricles)	11.1	22.7	22.2	0.5
Case 3 (Solid component)	9.0	30.9	30.0	0.9
Case 3 (Cystic component)	8.3	27.8	27.6	0.2

Table 2b: Print accuracy of 3D printed anatomical model (skull base)

	Skull (3D printed) (mm)	Skull (CT image) (mm)	Skull (3D printed with scaling)	Difference (mm)

			(mm)	
Case 1	56.8	114.8	113.6	1.2
Case 2	65.0	130.5	130.0	0.5
Case 3	38.0	128.0	126.7	1.3

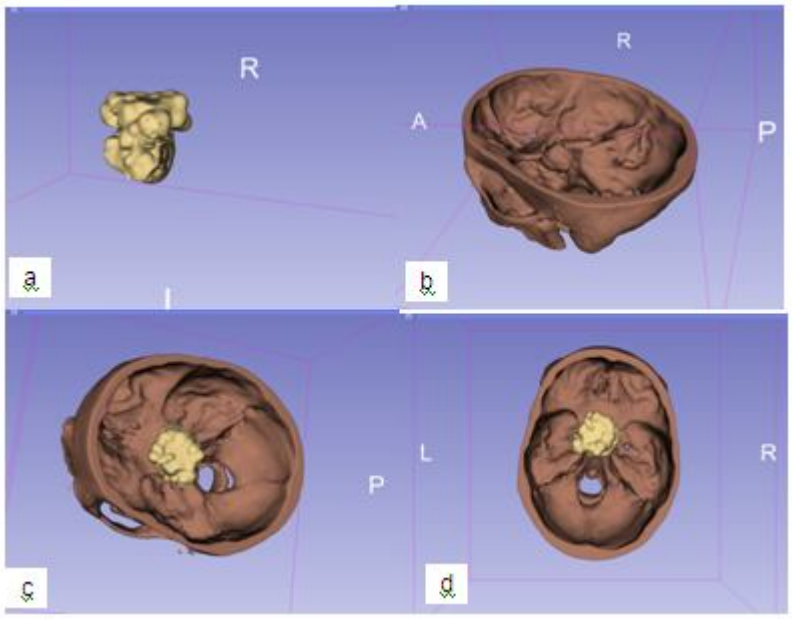

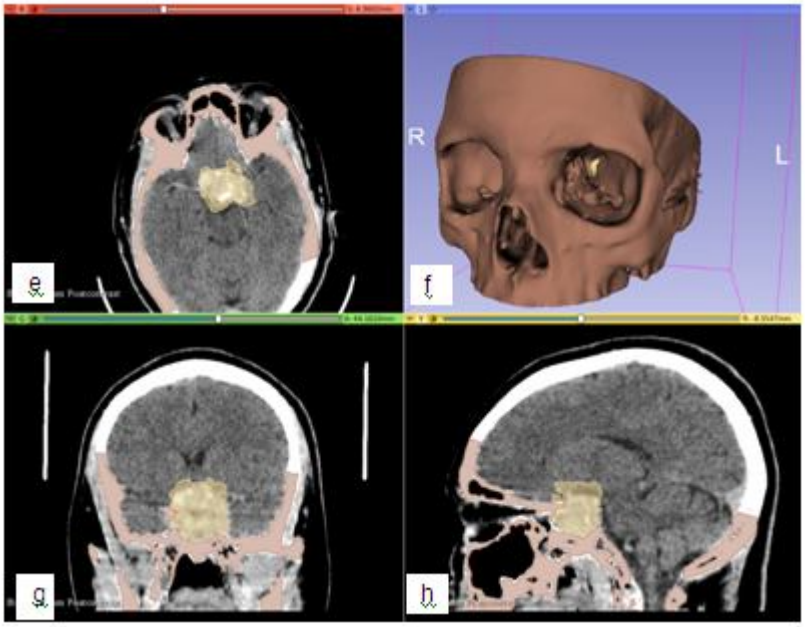

Figure 2: Case 1a-h. Lobulated mass in the pituitary fossa with 3D volume rendered images; the mass separately (a), pituitary fossa without the mass (b), mass in situ in the skull (c-d), facial bones (f), segmentation of mass on orthogonal CT stacks (e, g & h).

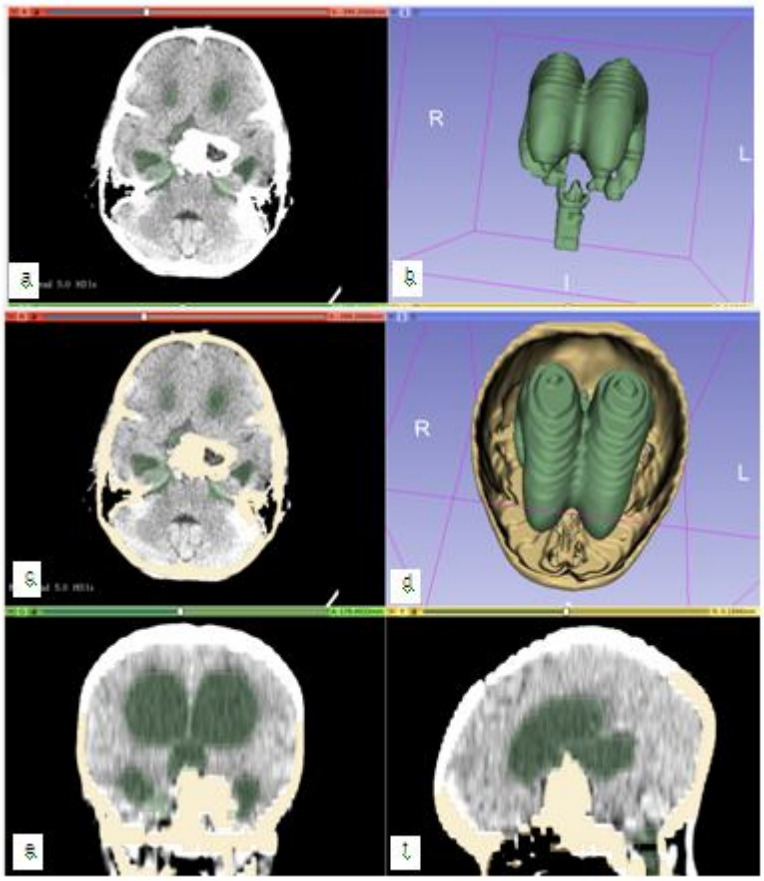

Figure 3: Case 2 a-f: Lobulated predominantly calcified mass in pituitary fossa. Axial, coronal, and sagittal CT Images showing dilated ventricles and calcified sellar mass (a, c, e & f). Segmented stacks with 3D volume rendered images of the dilated ventricles and skull (b & d).

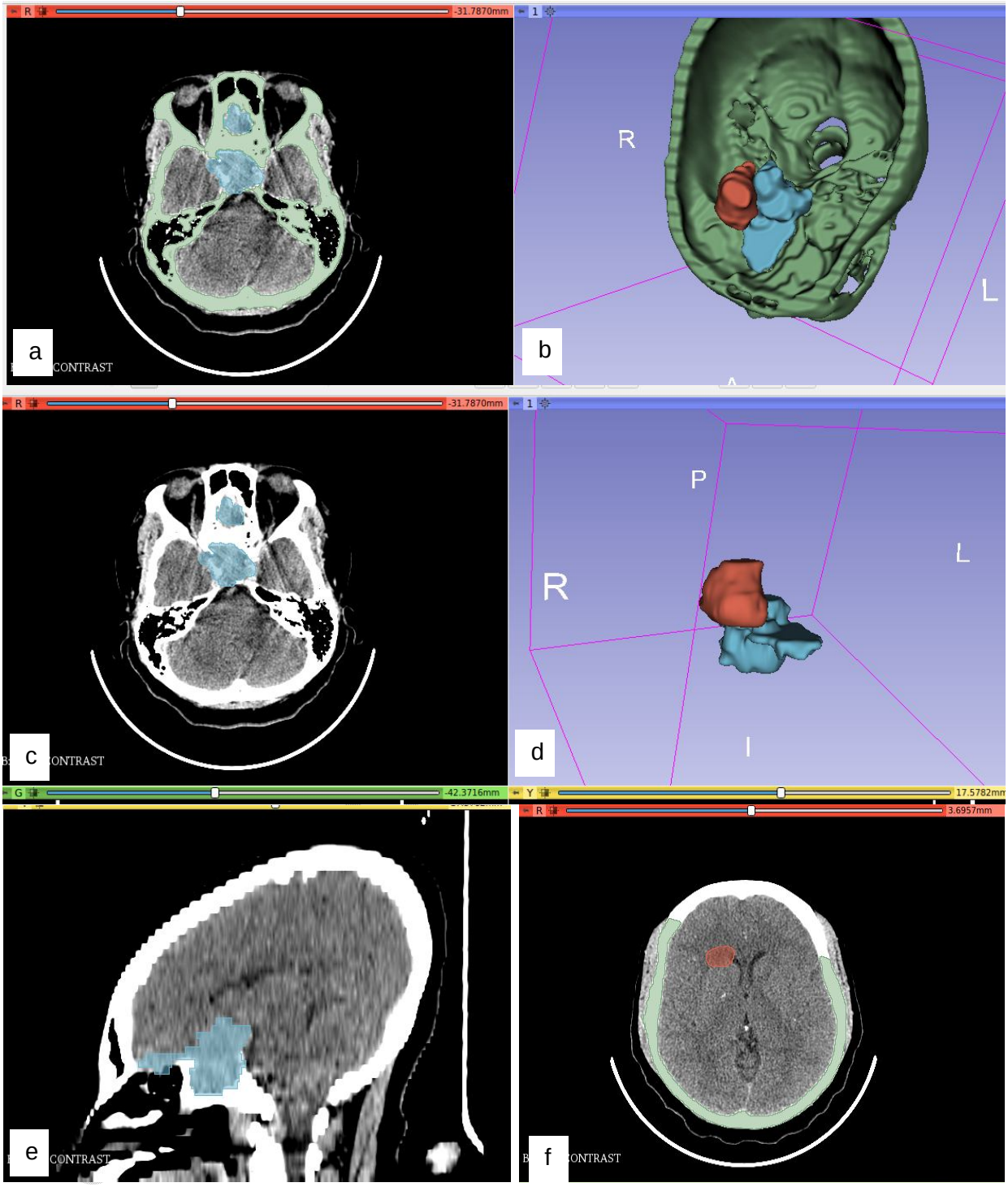

Figure 4 Case 3 a-f: Axial and sagittal Images showing irregularly shaped solid mass (blue) with calcifications arising from the sella with an adjacent cystic component (brown) extending into the suprasellar space (a, c & e) and into the right frontal lobe base (f) which was not so apparent on the CT stacks. Segmented and 3D volume rendered images of the mass and skull (b) and mass separately (d).

Figure 5: Case 1 Showing 3D printed loculated mass, skull base, and with a mass within the pituitary fossa

Figure 6: Case 2 Showing dilated ventricles, skull base and the calcified mass merging with the pituitary fossa (blue circle)

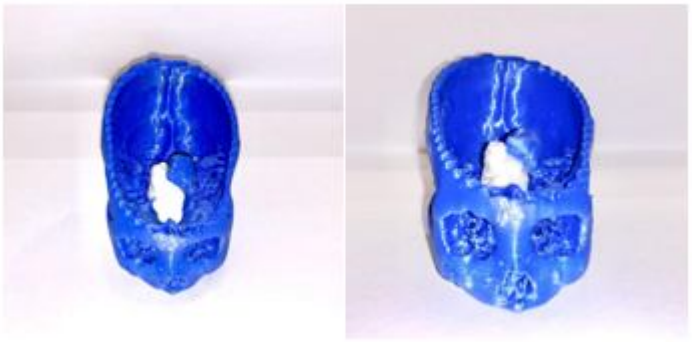

Figure 7: Case 3 Showing 3D printed loculated mass, skull base, and with a mass within the pituitary fossa

Table 3: Time of printing, segmentation, and cost analysis of each model

Case number	Time of segmentation (minutes)	Printing length (hours)	Amount of PLA filament used (grams)	Cost analysis of PLA filament used ($25/kg)	Personnel working cost	scaling
Case 1	45	9.25	36	$0.75	$23	0.5
Case 2	55	9	53	$1.1	$23	0.5
Case 3	90	4.25	16	$0.32	$46	0.3

Discussion

In this study, we identified the 3D printing workflow can be divided into five steps, similar to previous studies(15) and the stages were similar. This involves image acquisition from a cross-

sectional imaging to segmentation of the acquired DICOM image into a 3D model followed by file and model correction for final print, this is then followed on to slicing with the selection of 3D printing material as well as appropriate settings, this is then concluded with the actual print and print accuracy.

Segmentation of the structures of interest, particularly the tumour involves the use of drawing tools to manually segment the tumour(10) however, the process was aided by the use of contrast-enhanced images where the tumours tend to stand out due to contrast enhancement, and the presence of calcification as well made segmentation easier with use of semi-automatic tools like thresholding Use of artificial intelligence and deep learning approaches for automated classification and segmentation of head and neck cancers and brain tumours have been described and this can make this process automated in the future(16). This approach is however novel and was not employed in this study.

Bone was a very easy structure to segment when using segmentation tools and Hounsfield units(10). The bone is the most important aspect of the final model as it gives the relation of the tumour with the skull vault. It also shows infiltration by the tumour. In this study, we were able to identify bony destruction caused by the lesion and identify the lesion in relation to the skull.

The time it took to segment models differed depending on the complexity of the tumour in terms of its margins and borders. This ranged from 45-90 minutes, similar average times of segmentation have also been described in several studies(7,17) Use of FDM printers made it possible for models to be printed immediately as soon as the STL file models were available.

This is because FDM printers are commonly commercially available printers and was made available

Print accuracy was a consideration following prints of the models. It was observed that the print accuracy of all the anatomical models was less than 1.7mm (table 2). This is however not entirely surprising as FDM printers generally have a print accuracy of +/-0.5mm with mean errors of 0.44% (18,19).

The range exhibited could be from user bias in measuring, scaling, and also slicing thickness of images which lead to step ladder artifacts could have influenced measurement. The total time from the segmentation of images to 3D printing took an average of 8 hours. This further can give the impression of the possibility of having a point of care 3D printing of models that can be made available within 24-72 hours depending on the complexity of the case and skills involved.

Cost analysis is an important consideration especially if this is to be considered in a clinical setting. Cost analysis spans from time spent in development, cost of materials, and cost of 3D printers. This can be greatly influenced by the nature of lesion size, shape, and complexity in terms of mass infiltration. Another important consideration is the cost of the printer. But, considering this is a fixed item, the cost of the printer is not considered. The cost of each item is estimated during slicing which estimates the amount of PLA filament to be used in grams and metres. We were able to show that raw material printing cost is dependent on the scale of printing. In this study, the cost of PLA filament used per model was less than $1.2. In terms of personnel cost for segmentation, the time spent would determine the cost of segmentation

with a cost between $23 and $46 making the total cost less than $50 per model (table 3). This level of cost-effectiveness has been described in similar studies(7,17)

In conclusion, the researchers have shown it is possible to segment DICOM images of pituitary lesions and 3D print using an FDM printer with less than 1.7mm print accuracy. With this, we believe this can pave the way for point-of-care 3D printing for patients and clinicians when needed. The researchers have also done a cost analysis and shown it can be cost-effective as well.

Limitations of the study.

One major limitation in this study was poor contrast enhancement of carotid and cerebral arteries. Good segmentation of the cerebral arteries would have given more view of tumour's relationship with surrounding vessels. The use of one imaging modality, in this case, a CT scan machine was considered a limitation in this study. Other imaging modalities like MRI would have helped give a further and more detailed assessment of the tumours. In addition, this study was based on just 3 clinical cases, the use of more cases would have given more insight into factors that may affect accuracy.

A comprehensive study modelled on this work should be the obvious next step in making it very relevant to clinical practice, especially in sub-Saharan Africa.

Consent and ethical approval

As per international standards or university standard guidelines ethical approval has been collected and preserved by the authors.

References

1. John D. Carmichael. Overview of the Pituitary Gland - Hormonal and Metabolic Disorders [Internet]. MSD Manual Consumer Version. [cited 2022 Aug 30]. Available from: https://www.msdmanuals.com/en-gb/home/hormonal-and-metabolic-disorders/pituitary-gland-disorders/overview-of-the-pituitary-gland
2. Jones J, Datir A. Pituitary gland. Radiopaedia.org [Internet]. 2008 May 2 [cited 2022 Aug 30]; Available from: http://radiopaedia.org/articles/1888
3. Gaillard F, Weerakkody Y. Pituitary adenoma. Radiopaedia.org [Internet]. 2010 Oct 10 [cited 2022 Aug 30]; Available from: http://radiopaedia.org/articles/11024
4. Natarajan D, Tatineni S, Ponnapalli SP, Sachdeva V. Pituitary adenoma presenting as acute onset isolated complete third cranial nerve palsy without vision changes. BMJ Case Reports CP [Internet]. 2020 Jun 1 [cited 2022 Aug 30];13(6):e232490. Available from: https://casereports.bmj.com/content/13/6/e232490
5. Daly AF, Beckers A. The Epidemiology of Pituitary Adenomas. Endocrinol Metab Clin North Am. 2020 Sep 1;49(3):347–55.
6. Ezzat S, Asa SL, Couldwell WT, Barr CE, Dodge WE, Vance ML, et al. The prevalence of pituitary adenomas: a systematic review. Cancer [Internet]. 2004 Aug 1 [cited 2022 Aug 30];101(3):613–9. Available from: https://pubmed.ncbi.nlm.nih.gov/15274075/

7. Gillett D, Bashari W, Senanayake R, Marsden D, Koulouri O, MacFarlane J, et al. Methods of 3D printing models of pituitary tumors. 3D Print Med 2021 71 [Internet]. 2021 Aug 31 [cited 2022 Apr 22];7(1):1–14. Available from: https://threedmedprint.biomedcentral.com/articles/10.1186/s41205-021-00118-4
8. LAKE MG, KROOK LS, CRUZ S V. Pituitary Adenomas: An Overview. Am Fam Physician [Internet]. 2013 Sep 1 [cited 2022 Aug 30];88(5):319–27. Available from: https://www.aafp.org/pubs/afp/issues/2013/0901/p319.html
9. John A. Jane J, Catalino MP, Edward R. Laws J. Surgical Treatment of Pituitary Adenomas. Endotext [Internet]. 2022 Mar 9 [cited 2022 Aug 30]; Available from: https://www.ncbi.nlm.nih.gov/books/NBK278983/
10. Kamio T, Suzuki M, Asaumi R, Kawai T. DICOM segmentation and STL creation for 3D printing: a process and software package comparison for osseous anatomy. 3D Print Med 2020 61 [Internet]. 2020 Jul 31 [cited 2022 Aug 30];6(1):1–12. Available from: https://threedmedprint.biomedcentral.com/articles/10.1186/s41205-020-00069-2
11. Di Prima M, Coburn J, Hwang D, Kelly J, Khairuzzaman A, Ricles L. Additively manufactured medical products – the FDA perspective. 3D Print Med 2016 21 [Internet]. 2016 Dec 1 [cited 2022 Aug 30];2(1):1–6. Available from: https://threedmedprint.biomedcentral.com/articles/10.1186/s41205-016-0005-9
12. Volume Viewer | GE Healthcare (United States) [Internet]. [cited 2022 Aug 30]. Available from: https://www.gehealthcare.com/products/advanced-visualization/all-applications/volume-viewer
13. Snikhovska Kseniia. Seven Types of 3D Printers - Different printing and extruder

technologies [Internet]. 2022 [cited 2022 Aug 30]. Available from: https://penandplastic.com/3d-printer-types/

14. Gillett D, Bashari W, Senanayake R, Marsden D, Koulouri O, MacFarlane J, et al. Methods of 3D printing models of pituitary tumors. 3D Print Med 2021 71 [Internet]. 2021 Aug 31 [cited 2022 Aug 30];7(1):1–14. Available from: https://threedmedprint.biomedcentral.com/articles/10.1186/s41205-021-00118-4
15. Aimar A, Palermo A, Innocenti B. The Role of 3D Printing in Medical Applications: A State of the Art. J Healthc Eng. 2019;2019.
16. Badrigilan S, Nabavi S, Abin AA, Rostampour N, Abedi I, Shirvani A, et al. Deep learning approaches for automated classification and segmentation of head and neck cancers and brain tumors in magnetic resonance images: a meta-analysis study. Int J Comput Assist Radiol Surg [Internet]. 2021 Apr 1 [cited 2022 Aug 30];16(4):529–42. Available from: https://link.springer.com/article/10.1007/s11548-021-02326-z
17. Cost-effectiveness of 3d printing of anatomical models. Veterinaria. 2021;70(Suppl 1).
18. Petropolis C, Kozan D, Sigurdson L. Accuracy of medical models made by consumer-grade fused deposition modelling printers. Plast Surg [Internet]. 2015 [cited 2022 Aug 30];23(2):91. Available from: /pmc/articles/PMC4459415/
19. 3ERP. How dimensionally accurate are 3D printed parts? - 3ERP [Internet]. [cited 2022 Aug 30]. Available from: https://www.3erp.com/blog/how-dimensionally-accurate-are-3d-printed-parts/